Am J Transl Res 2022;14(9):6163-6174
www.ajtr.org /ISSN:1943-8141/AJTR0143354

Original Article

PPIB-regulated alternative splicing of cell cycle genes contributes to the regulation of cell proliferation

Yuan Zhang, Lei Liu, Minghui Zhou, Yujie Zhang, Hongxia Su, Dong Dong, Jia Wang

Department of Rhinology, The First Affiliated Hospital of Zhengzhou University, Zhengzhou 450052, Henan, People's Republic of China

Received April 6, 2022; Accepted July 30, 2022; Epub September 15, 2022; Published September 30, 2022

Abstract: Background: Peptidylprolyl cis-trans isomerase B (PPIB) plays an important role in the process of inflammation through binding RNA, but the molecular pathogenesis is not yet clearly understood. The objective of this study was to investigate and verify the PPIB-regulated gene expressions and alternative splicing in Hela cells. Methods: We examined the PPIB-regulated transcriptomes in HeLa cells using RNA-seq data. Differentially expressed genes, alternative splicing analysis were carried out. Functional enrichment analysis was used to define the enrichment of each term. Results: We found that PPIB knockdown successfully downregulated PPIB in Hela cells, which promoted cell proliferation ($P < 0.001$), but no significant effect on cell apoptosis. Ten alternative splicing genes regulated by PPIB were detected in Hela cells. The ten top Gene Ontology biological process analysis and functional pathways of the alternative splicing genes were screened and identified. The pathways where differentially expressed genes are most enriched were toll-like receptor 4 signaling pathways and other signaling pathways relating to inflammation and immune response. In addition, PPIB affects the alternative splicing of multiple genes, and the Gene Ontology-biological process analysis showed that genes significantly related to alternative splicing changes were mainly enriched in the cell cycle ($P < 0.05$). Conclusion: PPIB regulates the alternative splicing of cell cycle-related genes to affect cell proliferation and regulate the occurrence and development of chronic inflammatory diseases such as Nasal polyps.

Keywords: PPIB, nasal polyps, endoplasmic reticulum, RNA-seq

Introduction

Nasal polyposis (NP), a chronic inflammatory disease affecting the upper airways, is known to cause significant burden to quality of life, lead to significant health care expenditures and has been proved to have an impact on cognitive function [1-3]. NP affects almost 4% of population and is frequently associated with chronic lower airway disease with genetic or nongenetic origin [4]. Protein maturation in the endoplasmic reticulum (ER) needs proper folding, assembly and post-translational modifications [5], while the abnormal accumulation of unfolded or misfolded proteins at ER could lead to stressful situations of human diseases, including cancer, obesity and neurodegeneration. The ER proteostasis is mediated by the unfolded protein response (UPR), a signal transduction pathway that senses the fidelity of protein folding in the ER lumen [6, 7].

Cyclophilins are part of the immunophilin superfamily, which binds to the immunosuppressive drug cyclosporin as cell receptor proteins. Cyclophilins could catalyze the cis-trans isomerization of *xaa*-proline bonds, a rate-limiting step in protein folding, which is required for proteome homeostasis [8]. Peptidylprolyl cis-trans isomerase B (PPIB) is a functional peptidyl-prolyl cis/trans isomerase (PPIase), belonging to the cyclophilin family, regulates protein conformation of its substrates via prolyl cis-trans-isomerization in the ER lumen and nucleus, participates in protein folding, secretion and post-translational modification processes, and has multiple functions such as a novel regulator of endometrial cell proliferation and metastasis, taking part in sustaining normal growth and stress tolerance [9]. PPIB also play an important role in response to inflammatory stimuli and oxidative stress, participating in tissue or systemic inflammation [10]. In HEK293 and

HeLa cells, PPIB is believed to bind RNA and may be a new RNA binding protein (RBP) [8, 11]. During RNA transcription and post-transcriptional alternative splicing (AS), modification, transport, translation and degradation metabolism, a variety of specific RBPs bind to them for transcription and post-transcriptional regulation [12], and their expressions are abnormal or loss of function leading to the development of cancers and other diseases [13, 14]. For example, the biological role of 3-hydroxyacyl-CoA dehydrogenase type 2, which is considered as an unconventional RBP, has been characterized to regulate AS in the post-transcription [15]. Therefore, PPIB may affect the variable cleavage of RNA through its possible RBP function, thereby affecting the inflammatory response process and consequently the development and progression of nasal polyps. Previously studies have shown that PPIB acts as the UPR target proteins and are upregulated in NP tissues [16]. Moreover, oxidative stress induces UPR in human NP tissues and human nasal mucosal epithelial cells (HNEC), which in turn causes the secretion of inflammatory factors [17]. In the process of lipopolysaccharide-induced inflammatory response in macrophages, simultaneous administration of PPIB induces the expression of Bcl-3, reduces the expression of NF-α, and inhibits the inflammatory response [18]. In gastric cancer cells, PPIB and the pro-apoptotic factor CHOP are up-regulated by oxidative stress, and the inflammatory factor IL6 stimulates gastric cancer cells, which activates the JAK2/STAT3 signaling pathway and inhibits the expression of miR-520d-5p, while PPIB will further enhance the JAK2/STAT3 signaling pathway, thereby promoting the proliferation of gastric cancer cells [19]. In addition, PPIB interacts with E4 ligase P300 and then binds to CHOP to promote the phosphorylation and degradation of CHOP protein, thereby inhibiting the cell apoptosis induced by hypoxia [20]. However, the role of PPIB in NP is not yet fully understood. Hence, the objective of this study was to investigate and verify the PPIB-regulated gene expressions and AS in Hela cells.

Methods and materials

RNA extraction and sequencing

The sample names, description, the RNA-seq sequencing information were listed in Supplementary Table 1. Total RNA was extracted with TRIZOL (Ambion, USA). The RNA was further purified then treated with RQ1 DNase (Promega, Madison, USA) to remove DNA. The quality and quantity of the purified RNA were redetermined by measuring the absorbance at 260 nm/280 nm using Smartspec Plus (BioRad, USA).

For each sample, 1 μg of the total RNA was used for RNA-seq library preparation. Polyadenylated mRNAs were purified and fragmented, and then converted into double strand cDNA. After the step of end repair and A tailing, the DNAs were ligated to VAHTS RNA Adapters (Vazyme, China). Purified ligation products corresponding to 200-500 bps were digested with heat-labile UDG, and the single strand cDNA was amplified, purified, quantified and stored at -80°C before sequencing. For high-throughput sequencing, the libraries were prepared following the manufacturer's instructions and applied to Illumina HiSeq X Ten system for 150 nt paired-end sequencing.

RNA-Seq raw data clean and alignment

Raw reads containing more than 2-N bases were first discarded. Then adaptors and low-quality bases were trimmed from raw sequencing reads using FASTX-Toolkit (Version 0.0.13). Then, clean reads were aligned to the GRch38 genome by tophat2 allowing 4 mismatches [21]. Uniquely mapped reads were used for gene reads number counting and FPKM calculation (fragments per kilobase of transcript per million fragments mapped) [22].

Differentially expressed genes (DEGs) analysis and qRT-PCR validation of DEGs

The R Bioconductor package edgeR [23] was utilized to screen out the DEGs. A false discovery rate < 0.05 and fold change > 2 or < 0.5 were set as the cut-off criteria for identifying DEGs.

In this study, to elucidate the validity of the RNA-seq data, quantitative reverse-transcription polymerase chain reaction (qRT-PCR) was performed for some of the DEGs. The information of primers is presented in Supplementary Table 2. Total RNA remaining from RNA-seq library preparation was used for qRT-qPCR. RNA was reverse transcribed into cDNA using a M-MLV Reverse Transcriptase (Vazyme, China). Real-time PCR was performed with the StepOne

Table 1. Primer sets in this study

Gene	Primer	Sequence (5'-3')	Related figures
GAPDH	Forward	CGGAGTCAACGGATTTGGTCGTAT	**Figure 1A**
	Reverse	AGCCTTCTCCATGGTGGTGAAGAC	
PPIB	Forward	CCCAGTTCTTCATCACGACA	**Figure 1A**
	Reverse	GCTTCTCCACCTCGATCTTG	

RealTime PCR System using the SYBR Green PCR Reagents Kit (Yeasen, China). The PCR conditions were consisted of denaturing at 95°C for 10 min, 40 cycles of denaturing at 95°C for 15 s, annealing and extension at 60°C for 1 min. PCR amplifications were performed in triplicate for each sample. The RNA expression levels of all the genes were normalized against that of glyceraldehyde-3-phosphate dehydrogenase (GAPDH).

AS analysis

The AS events (ASEs) and regulated ASEs (RASEs) between the samples were defined and quantified by using the ABLas pipeline as described previously [8, 24]. In brief, ABLas detection of ten types of ASEs was based on the splice junction reads, including exon skipping (ES), alternative 5' splice site (A5SS), alternative 3'splice site (A3SS), intron retention (IR), mutually exclusive exons (MXE), mutually exclusive 5'UTRs (5pMXE), mutually exclusive 3'UTRs (3pMXE), cassette exon, A3SS&ES and A5SS&ES.

To assess RBP-RASEs, student's t-test was performed to evaluate the significance of the ratio alteration of ASEs. Those events which were significant at *P*-value cutoff corresponding to a false discovery rate cutoff of 5% were considered RBP-RASEs.

Construction of shPPIB vector

Sense and antisense strands were annealed to be shRNA. Vector pGFP-B-RS was digested by HindIII and BamHI at 37°C for 2 h-3 h. Then enzyme-digested vector was also run on 1.0% agarose gel and purified by Qiagen column kit. A linearized vector DNA digested by HindIII and BamHI and insert shRNA were catalyzed by T4 DNA Ligase (NEB). Plasmids were introduced into Escherichia coli by chemical transformation. Cells were plated onto LB plates containing kanamycin. The clates were then incubated overnight at 37°C. Colonies were screened by colony PCR (30 cycles) with universal primers (located on the backbone vector). The interference sequence of shRNA was verified by Sanger sequencing. shRNA target PPIB: GTTCTTCATCACGACAGTCAA.

Cell culture and transfections

Human CC (Cervical Carcinoma) cell lines, HeLa (CCTCC@GDC0009) cells were obtained from China Center for Type Culture Collection (Wuhan, Hubei, China). HeLa cells were cultured at 37°C with 5% CO_2 in Dulbecco's modified Eagle's medium (DMEM) with 10% fetal bovine serum (FBS), 100 μg/mL streptomycin, and 100 U/mL penicillin. Plasmid transfection of HeLa cells was performed using Lipofectamine 2000 (Invitrogen, Carlsbad, CA, USA) according to the manufacturer's protocol. Transfected cells were harvested after 48 h for RT-qPCR analysis.

Assessment of gene expression

GAPDH was used as a control gene for assessing the effects of PPIB knockdown. cDNA synthesis was done by standard procedures, and RT-qPCR was performed on the Bio-Rad S1000 with Bestar SYBR Green RT-PCR Master Mix (DBI Bioscience, Shanghai, China). The information of primers is presented in **Table 1**. The concentration of each transcript was then normalized to GAPDH mRNA level using $2^{-\Delta\Delta CT}$ method (Livak and Schmittgen 2001). Comparisons were performed by paired Student's t-test with the use of GraphPad Prism software (San Diego, CA).

Functional enrichment analysis

To sort out functional categories of DEGs, Gene Ontology (GO) terms and KEGG pathways were identified using KOBAS 2.0 server [25]. Hypergeometric test and Benjamini-Hochberg FDR controlling procedure were used to define the enrichment of each term.

Availability of data and materials

The data discussed in this study are available under GEO Series accession number GSE-188372. We also downloaded another published RNA-seq data of NP tissue from the patients with eosinophilic CRSwNP (n=3), noneosinophilic CRSwNP (n=3), and from healthy

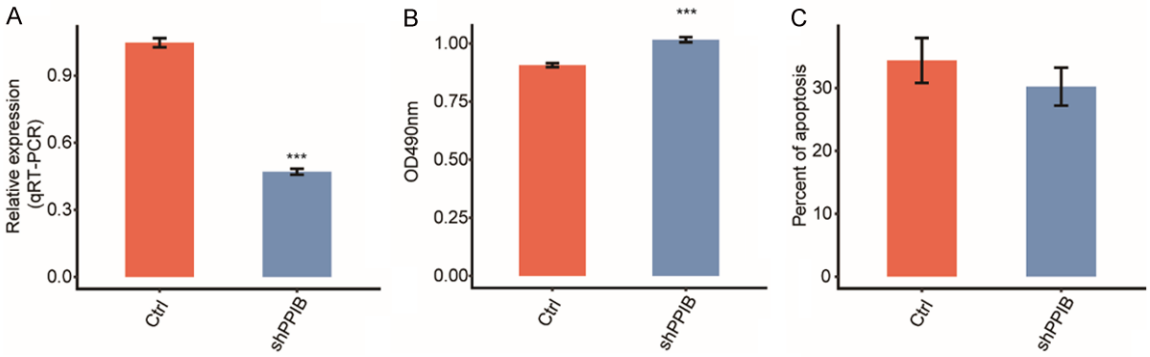

Figure 1. PPIB knockdown affects the proliferation of HeLa cells. A. PPIB expression quantified by qRT-PCR. B. MTT assay revealed that PPIB knockdown promoted cell proliferation in HeLa cells. C. Flow cytometric analysis revealed that PPIB knockdown had no significant effect on cell apoptosis. Error bars represent mean ± SEM. ***P < 0.001.

control subjects (n=3) (GSE72713) to analyze the ASEs between PPIB high expression and low expression samples.

Patients with NP and control individuals

In the experimental group, NP tissue specimens were obtained from 16 patients who underwent endoscopic NP resection in the First Affiliated Hospital of Zhengzhou University from January 2022 to July 2022. The patients were 21-66 years old, with 9 males and 7 females. Patients were excluded if they had allergic rhinitis, history of bronchial asthma or intolerance to aspirin. In the control group, inferior turbinate mucosa tissue samples were obtained from 16 patients with chronic hypertrophic rhinitis undergoing nasal endoscopic inferior turbinate mucosal resection in First Affiliated Hospital of Zhengzhou University during the same period. There were 8 males and 8 females, and they were 24 to 62 years old. This study was conducted in accordance with the Declaration of Helsinki and approved by the Medical Ethics Committee of First Affiliated Hospital of Zhengzhou University. Written informed consent was obtained from all the participants.

Statistical analysis

Statistical analysis was performed using SPSS software (version 18.0, Chicago, IL, USA). The measured data expressed as (mean ± standard deviation), were assessed by independent sample t-test. The correlation analysis was performed by Pearson test. Student's *t* test was performed to compare PPIB high and low groups with significance set at a *P* value of less than 0.05.

Results

PPIB knockdown affect the proliferation of HeLa cells

qRT-PCR indicated that PPIB knockdown (shPPIB) was downregulated compared with the control group (**Figure 1A**) ($p < 0.001$). MTT assay demonstrated that shPPIB promoted Hela cell proliferation (**Figure 1B**) ($P < 0.001$). However, flow cytometry showed no significant effect on apoptosis of Hela cells by shPPIB (**Figure 1C**).

Identification of PPIB-RASEs in HeLa cells

RNA-seq data were used to evaluate whether PPIB could regulate ASEs in Hela cells. The RNA-seq data further confirmed that the shPPIB was downregulated in Hela cells (**Figure 2A**). The ratio of exons of each RNA-seq sample were detected in genome annotation exons (**Figure 2B**). The number of known and novel identified splice junction of ctrl knockdown (shCtrl) and shPPIB were detected (**Figure 2C**). The number of known and novel ASEs for each type were distributed by using the ABLas pipeline (**Figure 2D**). RASE number of all ten AS genes regulated by PPIB were detected (**Figure 2E**).

Function analysis and validation of genes with PPIB-RASEs

The function and validation of genes with PPIB-RASEs were investigated. Data demonstrated

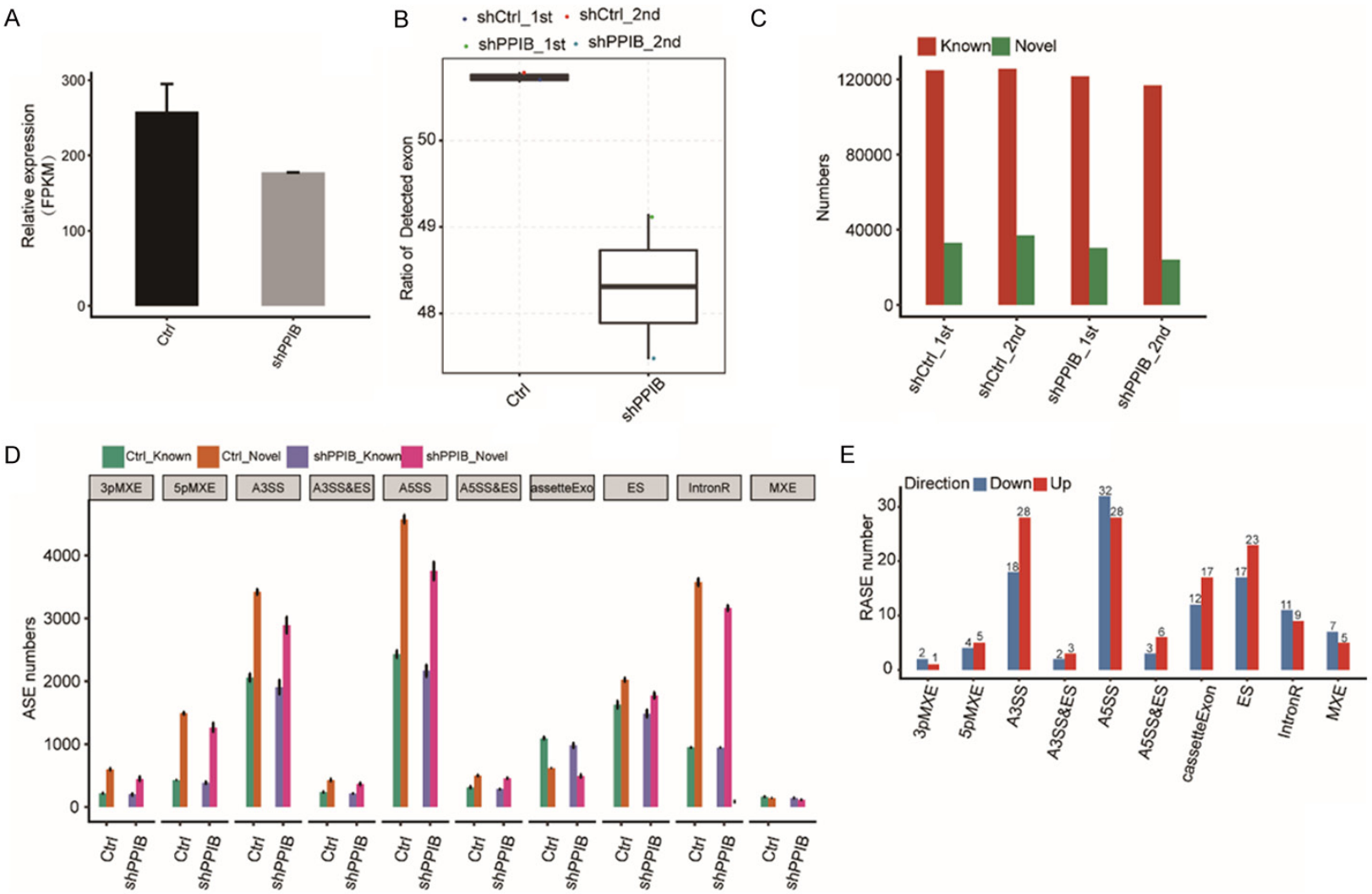

Figure 2. Identification of PPIB-regulated alternative splicing events (ASEs) in HeLa cells. A. PPIB expression quantified by RNA sequencing data. Error bars represent mean ± SEM. B. The ratio of exons detected in genome annotation exons for each RNA-seq sample. C. Number of known and novel identified splice junction for each sample. D. Distribution of known and novel ASEs for each type. E. Distribution of different AS types regulated by PPIB protein.

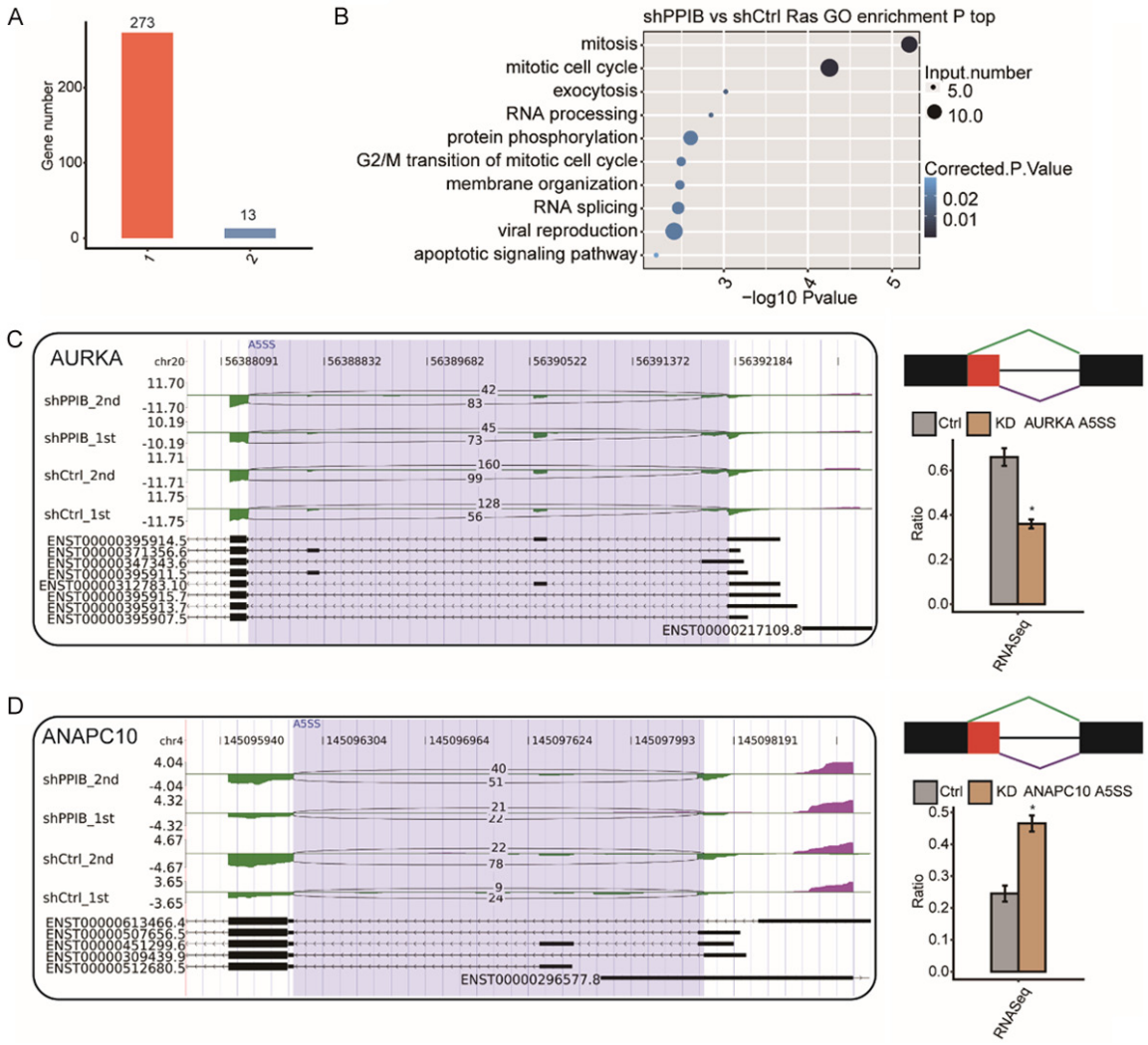

Figure 3. Identification and functional analysis of genes with PPIB-regulated alternative splicing events (ASEs). (A) Numbers of gene occurring one or more PPIB-regulated ASEs. (B) The top 10 GO biological process analysis functional pathways of the ASEs. The ASEs of AURKA (C) and ANAPC10 (D) regulated by PPIB were validated by schematic diagrams and qRT-PCR. The schematic diagrams depict the structures of ASEs, AS1 (purple line) and AS2 (green line). The exon sequences are denoted by boxes and intron sequences by the horizontal line (top panel). RNA-seq quantification ASEs are shown in the bottom panel. Error bars represent mean ± SEM. *p < 0.05, **p < 0.01. The altered ratio of ASEs in RNA-seq were calculated using the formula: AS1 junction reads/(AS1 junction reads + AS2 junction reads).

that the genes were associated with one or more PPIB-RASEs (**Figure 3A**). The top ten GO biological process analysis functional pathways of the AS genes were screened (**Figure 3B**). The ASEs of AURKA (**Figure 3C**) and ANAPC10 (**Figure 3D**) regulated by PPIB were validated by schematic diagrams and qRT-PCR ($P < 0.05$).

Identification and functional analysis of PPIB potentially regulated AESs in NP tissue

We then explore whether PPIB could regulate AESs in NP tissue. Using the downloaded transcriptome datasets, we analyzed the expression of PPIB in NP tissue from patients with eosinophilic (ECRSwNP) or noneosinophilic (non-ECRSwNP) chronic rhinosinusitis with NP and normal sinus mucosa (Ctrl) (**Figure 4A**). RASE number showed that the distribution of different AS types identified from different comparisons included ECRSwNP vs. Ctrl or non-ECRSwNP vs. Ctrl (**Figure 4B**). Further, the top 10 GO biological process terms of the AS genes were identified between ECRSwNP and Ctrl tissue (**Figure 4C**) and non-ECRSwNP and Ctrl (**Figure 4D**).

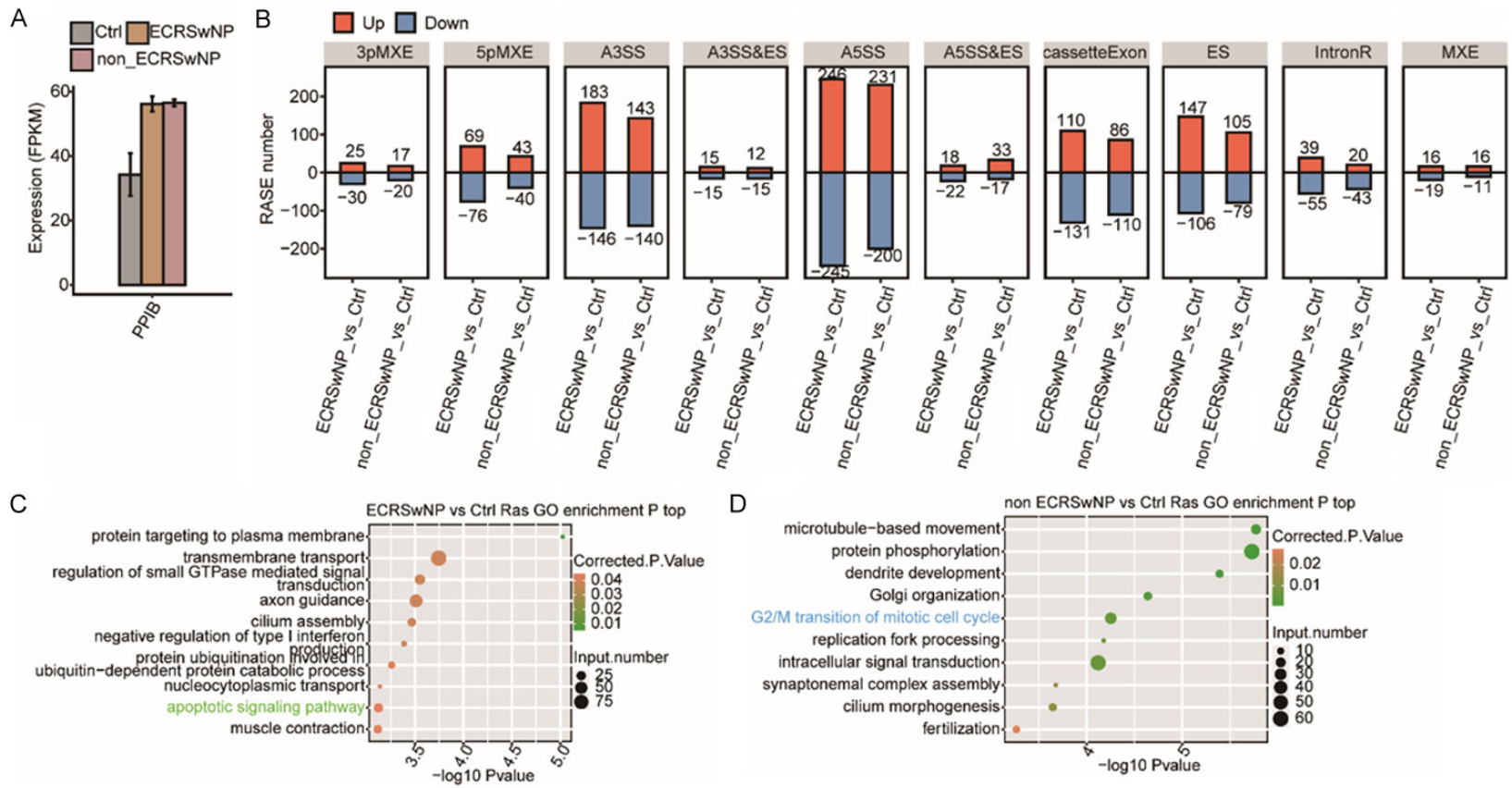

Figure 4. Identification and functional analysis of PPIB potentially regulated AS genes in NP tissue. A. Expression of PPIB in nasal polyp tissue from patients with eosinophilic (ECRSwNP) or noneosinophilic (non-ECRSwNP) chronic rhinosinusitis with nasal polyps and normal sinus mucosa (Ctrl) in the downloaded transcriptome datasets (GSE72713). B. Distribution of different AS types identified from different comparisons, ECRSwNP vs. Ctrl or non-ECRSwNP vs. Ctrl. C. The top 10 GO biological process terms of the alternative splicing genes identified between ECRSwNP and Ctrl tissue. D. The top 10 GO biological process terms of the alternative splicing genes identified between non-ECRSwNP and Ctrl.

PPIB potentially regulated AS of cell cycle associated genes in NP tissue

To determine whether PPIB could regulate AS of cell cycle associated gene in NP tissue, the overlap of PPIB-regulated AS genes (RASGs) between HeLa cells and NP tissue from ECRSwNP or non-ECRSwNP were conducted using Venn diagram (**Figure 5A**). Moreover, the common GO terms for PPIB-RASGs in HeLa cells and NP tissue from ECRSwNP or non-ECRSwNP were investigated (**Figure 5B**). A5SS event on NAA 60 (**Figure 5C**) and A3SS event on PSMD9 (**Figure 5D**) regulated by PPIB were validated by qRT-PCR ($P < 0.05$).

Validation the DEGs in NP patients

To validate the mentioned DEGs, the expression levels of the top 6 ones were further identified by qRT-PCR in our clinical samples. Similar to the above demonstrated results, the expression levels of AURKA, NAA60 and PSMD9 were significantly lower in NP tissue samples than in healthy individual samples (**Figure 6A**). In addition, the expression levels of ANAAPC10 and ANAAPC11 were significantly increased. While the expression of ANAPC15 showed no significant difference between the two groups (**Figure 6B**).

Discussion

To study the potential function of PPIB in inflammation, the PPIB-regulated transcriptomes in HeLa cells using RNA-seq data and PPIB-regulated gene expression and AS were conducted. Comparative transcriptome analysis revealed that knock-down of PPIB led to an extensive change of gene expression profiles and AS in HeLa cells. PPIB regulated the expression of ER proteins and might be affected by AS. After PPIB was knocked down in HeLa cells, the pathways where differentially expressed genes are most enriched were toll-like receptor 4 signaling pathways and other signaling pathways relating inflammation and immune response. Further, PPIB regulated the AS of multiple genes (Supplementary Figure 1) in NP tissue. The GO-biological process analysis of genes, which AS level changes significantly after PPIB silencing, is mainly enriched in the cell cycle. Therefore, PPIB not only participates in UPR's regulation of the expression of immune-inflammatory related genes and affects the inflammatory response, but also can regulate the AS of cell cycle-related genes to affect cell proliferation and regulate the occurrence and development of chronic inflammatory diseases such as NP.

Many types of RBPs can regulate AS, including the heterogeneous ribonucleoprotein (hnRNP) family of proteins, K homology domain, and other kinds of domains [26]. RNAi and CRISPR-Cas-mediated ablation of genes by genome-wide screening have identified a few hundred proteins that act directly or indirectly to regulate specific alternative exons [27, 28]. In this study, the PPIB knockdown has led to a great variety of RNA AS relating apoptosis process, gene expression, RNA splicing and other processes. Unlike PPIB commonly serves as PPIase activity which contributes to *Staphylococcus aureus* virulence or proteome homeostasis in *Burkholderia pseudomallei* [29, 30], the data in this study suggest that PPIB may affect cell proliferation by regulating the AS of cell cycle-related genes in ER, and this regulatory mechanism may also play an important role in the abnormal proliferation of cells in NP tissue via direct or indirect regulation pathway, although further research is needed.

We found that knockdown of PPIB in HeLa cells can affect the expression of ADRA1B, SLC6A12, NFE2, ATOH8 and other immune and inflammation-related genes, which proves that PPIB indeed participates in the regulation of inflammation. It is worth noting that knocking down PPIB can affect the RNA AS process (cell cycle, cell proliferation and protein phosphorylation) of pathway genes including SGK1, POM121, ANKLE2, and PDCD6. Interestingly, SGK1 protein has different splicing variants, and under hypoxic conditions, the expression of different splicing bodies will change [31], and SGK1 can participate in the regulation of cell proliferation by participating in protein phosphorylation and apoptosis process [32].

However, as there was no inflammation induction or activation of the ER stress response, the overall expression of these genes was low, but significant changes were still found. Therefore, it is necessary to verify the effect of PPIB on the expressions of these immune and inflammation-related genes under hypoxia or inflammation-induced conditions.

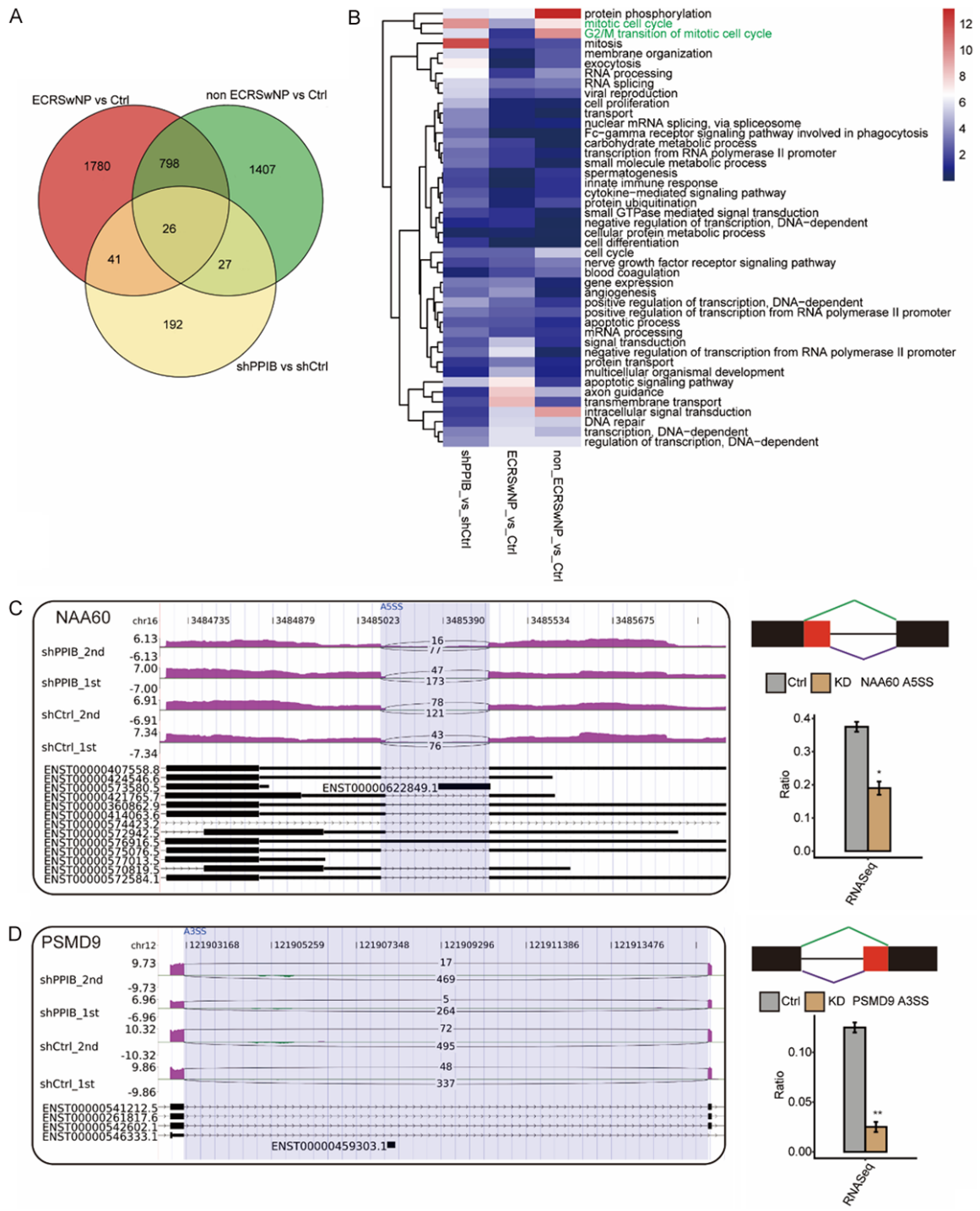

Figure 5. PPIB potentially regulated alternative splicing of cell cycle associated genes in NP tissue. (A) Venn diagram shows the result of overlap analysis of PPIB -regulated alternative splicing genes (RASGs) between HeLa cells and nasal polyp tissue from ECRSwNP or non-ECRSwNP. (B) The common GO terms for PPIBRASGs in HeLa cells and nasal polyp tissue from ECRSwNP or non-ECRSwNP. The color scale shows the significance (*p*-value) of the pathways. An A5SS event on NAA60 (C) and an A3SS event on PSMD9 (D) were shown. IGV-sashimi plots show the AS changes that occurred in HeLa cells after PPIB knockdown (left panel). The schematic diagrams depict the structures of ASEs (right panel, top), AS1 (shown in purple), and AS2 (shown in green); exon sequences are denoted by boxes, and intron sequences by the horizontal line. RNA-seq quantification of RASEs are shown (right panel, bottom). The altered ratio of RASEs was calculated using the formula: AS1 junction reads/AS1 junction reads + AS2 junction reads. Student's *t* test was performed to compare PPIB high and low groups with significance set at a *P* value of less than 0.05. **P* < 0.05, ***P* < 0.01, ***P* < 0.001.

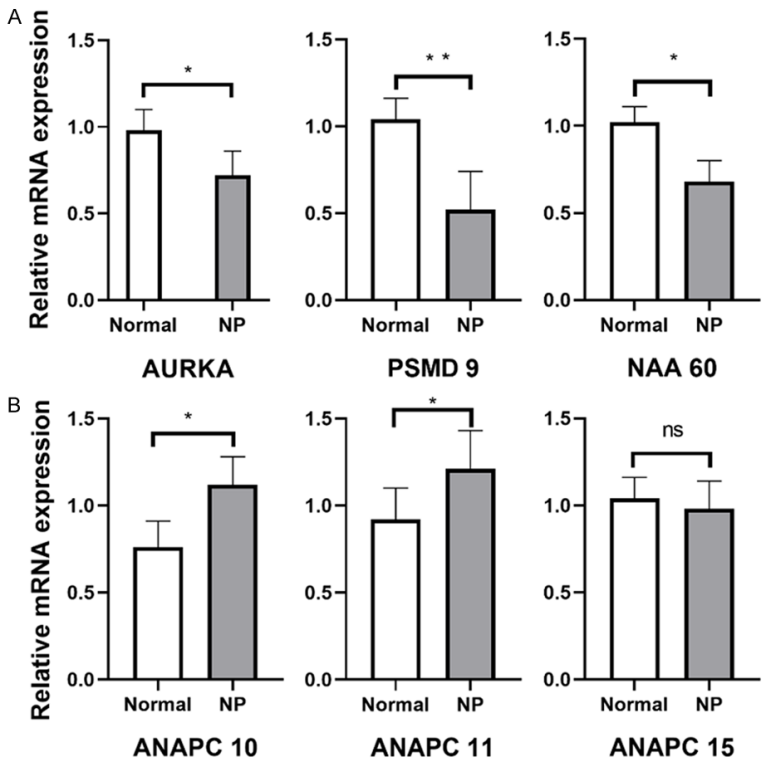

Figure 6. The expression of top 6 DEGs were measured in NP and healthy samples. A. mRNA expression of AURKA, NAA60 and PSMD9 were measured in NP tissue samples using qRT-PCR. B. RNA expression of ANAAPC10, ANAAPC11 and ANAAPC15 were measured in healthy samples. *P < 0.05, **P < 0.01.

Taken together, the data in this study support PPIB as a regulatory gene for the occurrence and development of chronic inflammatory diseases such as NP, further expand the understanding of regulatory functions and mechanisms in PPIB diseases and inflammation, and provide a theoretical basis for the development of therapeutic drugs for chronic inflammatory diseases such as NP.

Conclusions

PPIB regulate the AS of cell cycle-related genes to affect cell proliferation and regulate the occurrence and development of chronic inflammatory diseases such as NP.

Disclosure of conflict of interest

None.

Address correspondence to: Yuan Zhang, Department of Rhinology, The First Affiliated Hospital of Zhengzhou University, Zhengzhou 450052, Henan, People's Republic of China. Tel: +86-0371-67967271; E-mail: zhangyuanzzuedu@163.com

References

[1] Soler ZM, Sauer D, Mace J and Smith TL. Impact of mucosal eosinophilia and nasal polyposis on quality-of-life outcomes after sinus surgery. Otolaryngol Head Neck Surg 2010; 142: 64-71.

[2] Erskine SE, Hopkins C, Clark A, Anari S, Robertson A, Sunkaraneni S, Wilson JA, Beezhold J and Philpott CM. Chronic rhinosinusitis and mood disturbance. Rhinology 2017; 55: 113-119.

[3] Fokkens W, Van Der Lans R and Reitsma S. Dupilumab for the treatment of chronic rhinosinusitis with nasal polyposis. Expert Opin Biol Ther 2021; 21: 575-585.

[4] Bachert C, Hormann K, Mosges R, Rasp G, Riechelmann H, Muller R, Luckhaupt H, Stuck BA and Rudack C. An update on the diagnosis and treatment of sinusitis and nasal polyposis. Allergy 2003; 58: 176-191.

[5] Ellgaard L and Helenius A. Quality control in the endoplasmic reticulum. Nat Rev Mol Cell Biol 2003; 4: 181-191.

[6] Hetz C, Zhang K and Kaufman RJ. Mechanisms, regulation and functions of the unfolded protein response. Nat Rev Mol Cell Biol 2020; 21: 421-438.

[7] Walter P and Ron D. The unfolded protein response: from stress pathway to homeostatic regulation. Science 2011; 334: 1081-1086.

[8] Zhu Y, Gong Y, Li A, Chen M, Kang D, Liu J and Yuan Y. Differential proteomic analysis reveals protein networks and pathways that may contribute to helicobacter pylori FKBP-type PPIase-associated gastric diseases. Proteomics Clin Appl 2018; 12: e1700127.

[9] Liu J, Zuo Y, Qu GM, Song X, Liu ZH, Zhang TG, Zheng ZH and Wang HK. CypB promotes cell proliferation and metastasis in endometrial carcinoma. BMC Cancer 2021; 21: 747.

[10] Zhang H, Fan Q, Xie H, Lu L, Tao R, Wang F, Xi R, Hu J, Chen Q, Shen W, Zhang R and Yan X.

Elevated serum cyclophilin B levels are associated with the prevalence and severity of metabolic syndrome. Front Endocrinol (Lausanne) 2017; 8: 360.
[11] Baltz AG, Munschauer M, Schwanhausser B, Vasile A, Murakawa Y, Schueler M, Youngs N, Penfold-Brown D, Drew K, Milek M, Wyler E, Bonneau R, Selbach M, Dieterich C and Landthaler M. The mRNA-bound proteome and its global occupancy profile on protein-coding transcripts. Mol Cell 2012; 46: 674-690.
[12] Hentze MW, Castello A, Schwarzl T and Preiss T. A brave new world of RNA-binding proteins. Nat Rev Mol Cell Biol 2018; 19: 327-341.
[13] Holmqvist E and Vogel J. RNA-binding proteins in bacteria. Nat Rev Microbiol 2018; 16: 601-615.
[14] Turner M and Diaz-Munoz MD. RNA-binding proteins control gene expression and cell fate in the immune system. Nat Immunol 2018; 19: 120-129.
[15] Tejedor JR, Papasaikas P and Valcarcel J. Genome-wide identification of Fas/CD95 alternative splicing regulators reveals links with iron homeostasis. Mol Cell 2015; 57: 23-38.
[16] Mujcic H, Rzymski T, Rouschop KM, Koritzinsky M, Milani M, Harris AL and Wouters BG. Hypoxic activation of the unfolded protein response (UPR) induces expression of the metastasis-associated gene LAMP3. Radiother Oncol 2009; 92: 450-459.
[17] Jeanson L, Kelly M, Coste A, Guerrera IC, Fritsch J, Nguyen-Khoa T, Baudouin-Legros M, Papon JF, Zadigue P, Pruliere-Escabasse V, Amselem S, Escudier E and Edelman A. Oxidative stress induces unfolding protein response and inflammation in nasal polyposis. Allergy 2012; 67: 403-412.
[18] Marcant A, Denys A, Melchior A, Martinez P, Deligny A, Carpentier M and Allain F. Cyclophilin B attenuates the expression of TNF-alpha in lipopolysaccharide-stimulated macrophages through the induction of B cell lymphoma-3. J Immunol 2012; 189: 2023-2032.
[19] Li T, Guo H, Zhao X, Jin J, Zhang L, Li H, Lu Y, Nie Y, Wu K, Shi Y and Fan D. Gastric cancer cell proliferation and survival is enabled by a cyclophilin B/STAT3/miR-520d-5p signaling feedback loop. Cancer Res 2017; 77: 1227-1240.
[20] Jeong K, Kim H, Kim K, Kim SJ, Hahn BS, Jahng GH, Yoon KS, Kim SS, Ha J, Kang I and Choe W. Cyclophilin B is involved in p300-mediated degradation of CHOP in tumor cell adaptation to hypoxia. Cell Death Differ 2014; 21: 438-450.
[21] Kim D, Pertea G, Trapnell C, Pimentel H, Kelley R and Salzberg SL. TopHat2: accurate alignment of transcriptomes in the presence of insertions, deletions and gene fusions. Genome Biol 2013; 14: R36.
[22] Trapnell C, Williams BA, Pertea G, Mortazavi A, Kwan G, van Baren MJ, Salzberg SL, Wold BJ and Pachter L. Transcript assembly and quantification by RNA-Seq reveals unannotated transcripts and isoform switching during cell differentiation. Nat Biotechnol 2010; 28: 511-515.
[23] Robinson MD, McCarthy DJ and Smyth GK. edgeR: a bioconductor package for differential expression analysis of digital gene expression data. Bioinformatics 2010; 26: 139-140.
[24] Jin L, Li G, Yu D, Huang W, Cheng C, Liao S, Wu Q and Zhang Y. Transcriptome analysis reveals the complexity of alternative splicing regulation in the fungus verticillium dahliae. BMC Genomics 2017; 18: 130.
[25] Xie C, Mao X, Huang J, Ding Y, Wu J, Dong S, Kong L, Gao G, Li CY and Wei L. KOBAS 2.0: a web server for annotation and identification of enriched pathways and diseases. Nucleic Acids Res 2011; 39: W316-322.
[26] Lunde BM, Moore C and Varani G. RNA-binding proteins: modular design for efficient function. Nat Rev Mol Cell Biol 2007; 8: 479-490.
[27] Han H, Braunschweig U, Gonatopoulos-Pournatzis T, Weatheritt RJ, Hirsch CL, Ha KCH, Radovani E, Nabeel-Shah S, Sterne-Weiler T, Wang J, O'Hanlon D, Pan Q, Ray D, Zheng H, Vizeacoumar F, Datti A, Magomedova L, Cummins CL, Hughes TR, Greenblatt JF, Wrana JL, Moffat J and Blencowe BJ. Multilayered control of alternative splicing regulatory networks by transcription factors. Mol Cell 2017; 65: 539-553, e537.
[28] Gonatopoulos-Pournatzis T, Wu M, Braunschweig U, Roth J, Han H, Best AJ, Raj B, Aregger M, O'Hanlon D, Ellis JD, Calarco JA, Moffat J, Gingras AC and Blencowe BJ. Genome-wide CRISPR-Cas9 interrogation of splicing networks reveals a mechanism for recognition of autism-misregulated neuronal microexons. Mol Cell 2018; 72: 510-524, e512.
[29] Keogh RA, Zapf RL, Wiemels RE, Wittekind MA and Carroll RK. The Intracellular cyclophilin PpiB contributes to the virulence of staphylococcus aureus independently of its peptidyl-prolyl cis/trans isomerase activity. Infect Immun 2018; 86: e00379-18.
[30] Bzdyl NM, Scott NE, Norville IH, Scott AE, Atkins T, Pang S, Sarovich DS, Coombs G, Inglis TJJ, Kahler CM and Sarkar-Tyson M. Peptidyl-Prolyl Isomerase ppiB Is essential for proteome homeostasis and virulence in burkholderia pseudomallei. Infect Immun 2019; 87: e00528-19.

[31] Simon P, Schneck M, Hochstetter T, Koutsouki E, Mittelbronn M, Merseburger A, Weigert C, Niess A and Lang F. Differential regulation of serum- and glucocorticoid-inducible kinase 1 (SGK1) splice variants based on alternative initiation of transcription. Cell Physiol Biochem 2007; 20: 715-728.

[32] Bai JA, Xu GF, Yan LJ, Zeng WW, Ji QQ, Wu JD and Tang QY. SGK1 inhibits cellular apoptosis and promotes proliferation via the MEK/ERK/p53 pathway in colitis. World J Gastroenterol 2015; 21: 6180-6193.

Supplementary Table 1. Summary of sample names, description, the RNA-seq sequencing information and mapping results in each sample

Sample	Description	Total clean reads	Total mapped	Total Uniquely mapped	Splice reads	Non-splice reads
shCtrl_1st	control_1	86378188	51755562 (59.92%)	47142331 (91.09%)	23499446 (49.85%)	23642885 (50.15%)
shCtrl_2nd	control_2	89834074	61998584 (69.01%)	58070270 (93.66%)	30269177 (52.13%)	27801093 (47.87%)
shPPIB_1st	PPIB_knockdown_1	80395764	58118992 (72.29%)	53464120 (91.99%)	27789043 (51.98%)	25675077 (48.02%)
shPPIB_2nd	PPIB_knockdown_2	84720448	59495478 (70.23%)	54683975 (91.91%)	28684275 (52.45%)	25999700 (47.55%)

Supplementary Table 2. Primer information sets in **Figure 6**

Gene	Primer	Sequence (5'-3')
GAPDH	Forward	TCCTGCACCACCAACTGCTTA
	Reverse	AGTGATGGCATGGACTGTGGT
AURKA	Forward	GTGCATGCTCCATCTTCCAG
	Reverse	AGTCTCCTGGTACGTGTGTG
ANAAPC10	Forward	TCAGGCTGTYTGGTCACTCT
	Reverse	AGCCATCRGATTGCCAGTAA
NAA60	Forward	GAATCTTCCTTAACGGAGC
	Reverse	AAGAGACTTGATCTTTCGGT
PSMD9	Forward	AAGGCCAACTATGACGTGCTG
	Reverse	ATATGATGTTGTGCCTGGCG
ANAPC11	Forward	ATGAAGGTGAAGATTAAGT
	Reverse	TCACTCCTTGAACTTCCATT
ANAPC15	Forward	ACTCTACCCTGCTTATTGCCCG
	Reverse	CACCATGTGCTCATCAAAGCCG

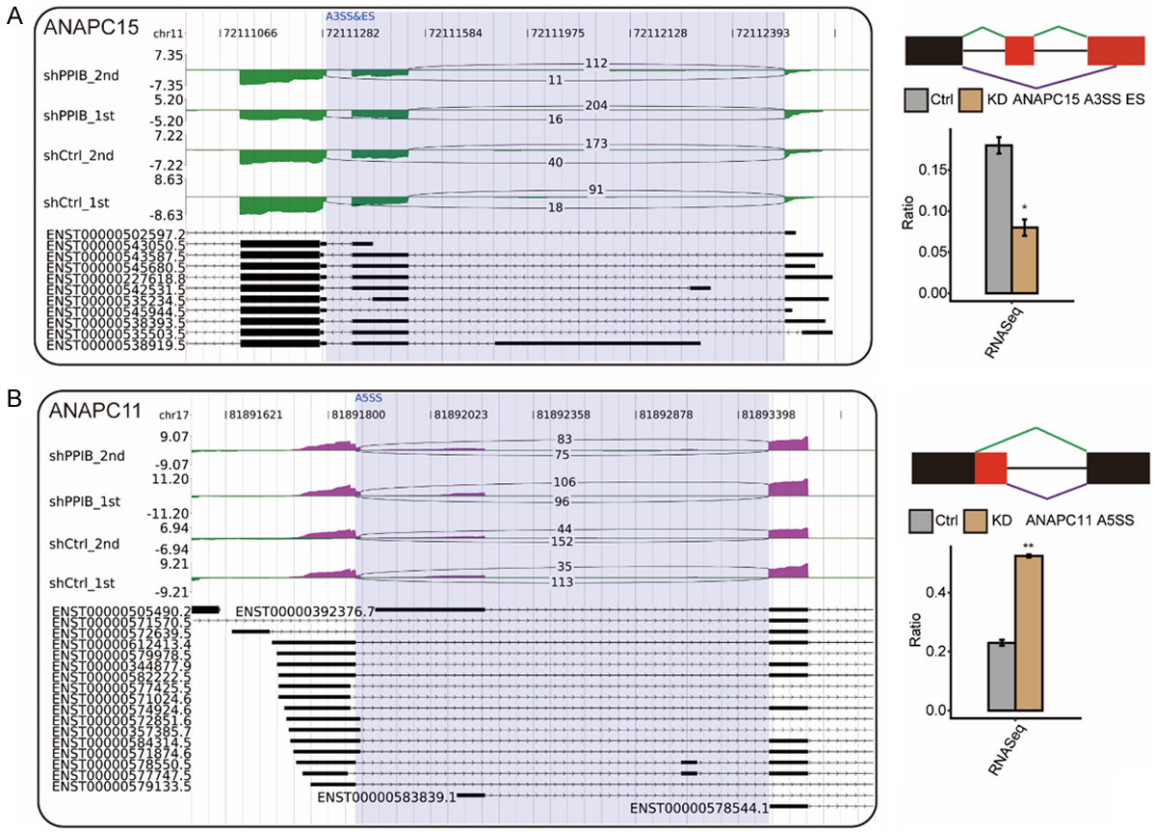

Supplementary Figure 1. PPIB potentially regulated AS of cell cycle associated genes in NP tissue. An A3SS event on ANAPC15 (A) and an A5SS event on ANAPC10 (B) were shown. IGV-sashimi plots show the alternative splicing changes that occurred in HeLa cells after PPIB knockdown (left panel). The schematic diagrams depict the structures of ASEs (right panel, top), AS1 (shown in purple) and AS2 (shown in green); exon sequences are denoted by boxes, and intron sequences by the horizontal line. RNA-seq quantification of RASEs are shown (right panel, bottom). The altered ratio of RASEs was calculated using the formula: AS1 junction reads/AS1 junction reads + AS2 junction reads. Student's t test was performed to compare PPIB high and low groups with significance set at a *P* value of less than 0.05. *P < 0.05, **P < 0.01, **P < 0.001.